HF Propagation Measurement Techniques and Analyses

Steve Cerwin WA5FRF

This paper presents methods and equipment for performing HF skywave propagation measurements using WWV standard time and frequency stations and selected results. Topics include single frequency and spectral analysis methods for measurement of ionospherically induced Doppler shifts, comparison of WWV frequency data taken simultaneously on multiple frequencies, observation of skywave mode splitting during the dawn and dusk day/night transitions, the use of precise WWV timing tick measurements to identify single and multihop propagation modes, and techniques for separating WWV and WWVH during simultaneous reception. Instrumentation methods, data records, and propagation insights are given.

I. Introduction

The author participated in the HamSCI effort to measure the impact of the 2017 North American total eclipse on LF and HF propagation by recording amplitude data on both 5 MHz WWV and 60 kHz WWVB. Subsequently, as a calibration procedure for an ARRL Frequency Measuring Test the author recorded detailed on-air WWV spectrograms .[1] In the process of monitoring the apparent frequency of 5 MHz WWV over a CO to TX path several interesting frequency effects were observed. Over several days of observation the general frequency behavior was observed to be turbulent at night and steady during the day. The transition from night to day at dawn was marked by a comparatively large positive frequency swing while the transition from day to night at dusk showed a complimentary negative swing. Additionally, the frequency track at sunrise was observed to diverge into multiple higher order tracks that progressed geometrically upwards in frequency. On some occasions the higher order modes were continuous throughout the night-day transition but on others some higher order modes would manifest abruptly midway through the transition. The evening negative swing occasionally broke into multiple tracks but generally was more docile than the dawn behavior.

This paper describes measurement techniques and experiments designed to learn more about these phenomena. Experimental procedures, data records, and possible inferences to ionospheric physics are given in the following sections.

II. Ionospherically Induced Frequency Variations

A. Instrumentation for Frequency Measurements

The ionospherically induced frequency shifts are very small compared to the HF carrier frequency. Nighttime turbulence may be only a few tenths of a Hz in amplitude and the peak swings at dawn and dusk can reach 1-3 Hz. A typical communications receiver with digital frequency readout has neither the display resolution nor the means to determine the precise frequency of a received carrier with the required accuracy. So the usual procedure is to place the receiver in Upper Side Band (USB) mode and tune it low in frequency so that the difference between the receiver and actual frequency comes out as a tone in the audio output. In essence, the process frequency-translates the carrier frequency from RF to audio. The translation preserves minute frequency variations and places them about a drastically reduced center frequency. This allows analysis on a computer based spectrum analyzer using a sound card. A common setup uses 1000 Hz as the tone frequency. The receiver is set for 4.999 MHz in USB mode for 5 MHz WWV. The spectrum analyzer program is set up with a 1000 Hz center frequency with a 10 Hz span. This allows resolution down to about 10 milliHertz (mHz).

Not all receivers are suitable for high precision frequency measurements because they do not possess the required long and short term frequency stability. The frequency specifications for accuracy and stability for many receivers is on the order of 5-10 HZ, which is fine for all normal

[1] Ionospheric Disturbances at Dawn, Dusk, and During the 2017 Eclipse. Steve Cerwin WA5FRF. QEX, Sept/Oct 2018

amateur radio modes but may not be good enough if the receiver does not settle down after a lengthy warm up. One way to tell if a receiver is usable is to watch the mid-day propagation of 5 MHz WWV since it usually shows flat frequency characteristics. Even good receivers require lengthy warm up times (> 6 hours) in a temperature stabilized room. But even then day-long records have dubious frequency track accuracy if precision to 0.1 Hz or better is desired. A far better approach for receivers that will accept an external reference is to stabilize the receiver with a GPS Disciplined Oscillator (GPSDO). These devices have become readily and inexpensively available. They put out a 10 MHz reference clock and a 1 pps reference with accuracy and stability that are comparable to WWV itself. The author's Icom IC-7610 and R8600 were stabilized in this way.

Another measurement issue is ensuring a high fidelity audio connection between the receiver and the computer sound card. Simply connecting the audio output of the radio to the audio in of the computer can lead to serious ground loop problems. Induced currents from the AC mains and computer switching power supplies can distort and even obliterate the desired signal. The solution is to break the connection with transformer coupling. All of the data presented here used a 600:600 ohm isolation transformer with impedance matching and level control circuitry. The primary side connected to the radio used a 560 ohm series resistor to set a nominal 600 ohm input impedance to the transformer. The secondary was connected across a 1k ohm pot with the wiper ported to the sound card input to provide a separate level control. Finally care must be taken not to overdrive the audio circuitry or harmonic and intermodulation distortion will result.

The spectral waterfall plots were captured using Spectrum Lab, a versatile spectrum analysis program available on the internet. The DSP parameters were selected for the task at hand and varied according to desired record length, update rate, spectral resolution, and desired analog dynamic range. Input levels to the sound card were set using the receiver volume control and the inline isolation circuit. Recording levels in Spectrum Lab were usually set up for a -10 to -60 dBfs range, for a 50 dB display range. A Hamming window function was used with a 75% overlap. Figure 1 shows the DSP parameters used for Fast, Moderate, and Slow data acquisition times. Columns 2-4 are user inputs entered into the program and the remaining columns show the resulting data acquisition parameters.

Acquisition Time	Sample rate	Decimate Divisor	FFT length	Sample Rate-kSPS	FFT Bin mHz	Noise BW mHz	Max Freq kHz	FFT Window Time	Update Rate-sec	Waterfall Increment
Fast	44100	8	65536	5.51222	84.1099	114.389	2.75611	11.89 sec	2.9725	5 min
Fast	44100	16	65536	2.75611	42.0549	57.1947	1.37806	23.78 sec	5.945	5 min
Fast	44100	8	131072	5.51222	42.0549	57.1947	2.75611	23.78 sec	5.945	5 min
Moderate	44100	12	131072	3.67482	28.0366	38.1298	1.83741	35.67 sec	8.9175	15 min
Moderate	44100	16	131072	2.75611	21.0275	28.5974	1.37806	47.56 sec	11.89	15 min
Slow	44100	16	262144	2.75611	10.5137	14.2987	1.37806	1.585 min	23.775	30 min
Slow	11025	4	524288	2.75625	5.25713	7.1497	1.37813	3.17 min	47.55	1 hr.

Figure 1 Spectrum Lab DSP Parameters Used in the Study

B. Measured Spectrograms

1. Typical Diurnal Behavior at 5 MHz

Figure 2 shows typical behavior of 5 MHz WWV over periods of time that include night, day, and the morning and evening transition periods. This data was taken with a thoroughly warmed up and stable receiver but without a GPSDO, so only relative and not absolute frequency is calibrated. The spectrogram is a waterfall display with oldest data at the bottom and newest at the top. The scale factor is 1 Hz/div horizontal and 1 hr./div vertical. At night the carrier frequency shows considerable turbulence with peak to peak values reaching 0.5 Hz. During the day, the turbulence disappears and the frequency track virtually straight-lines. The negative frequency swing as day transitions to night is clearly evident in the top half of the figure. This transition is relatively docile compared to wild frequency swings at dawn shown on the bottom half. The sunrise transition shows an intermittent mode with virtually no frequency shift, a continuous higher order frequency shift, and two additional higher order modes that manifest abruptly midway through the transition.

2. Simultaneous 2.5, 5, and 10 MHz records

Additional data were taken shortly after the HamSCI Festival of Frequency Measurements commemorating the WWV Centennial. Figures 3 through 5 show simultaneous recordings of 2.5, 5, and 10 MHz WWV. The data spans a time from 2100z on Oct. 10, 2019 through1800z on Oct. 13, 2019. The receiver for 10 MHz was marginal on long term stability so some of the gradual drift shown in the spectrogram may have been receiver drift. As before horizontal scale is 1 Hz/div and vertical is 1 hr./div. A number of features correlate across frequency while others do not. All traces show positive frequency swings at dawn and negative swings at dusk, though to varying degrees and with varying characteristics. These Doppler shifts result from the velocity of path length changes as ionization layers descend at dawn and ascend at dusk. One interesting difference is that both 2,5 and 5 MHz show turbulent frequency behavior only at night whereas 10 MHz shows turbulence both day and night. This may have interesting implications for D layer absorption, reach into the upper ionosphere, and where the turbulence actually takes place. Another difference is that both 2.5 and 5 MHz show mode splitting at dawn whereas 10 MHz does not. This may have implications for multiple hop propagation and the inability of 10 MHz to support the high angle of propagation required for a multiple hop mode. The 10 MHz spectrogram also showed an interesting parallel frequency track from 0100z to 0900z on Oct. 13, 2019. The parallel track was displaced high in frequency by 1.5-2 Hz.

The fact that the nighttime frequency turbulence does not scale with operating frequency is interesting. Pure Doppler shifts or wave speed accelerations should scale with carrier frequency. So if all three frequencies were subjected to the same Doppler velocity the frequency shift at 5 MHz should be twice that at 2.5 MHz, and the shift at 10 MHz twice that. Yet the magnitude of the turbulence was about the same for all three frequencies. It appears that unless there is an offsetting effect that diminishes interaction with increasing frequency the cause for the turbulence may be something else.

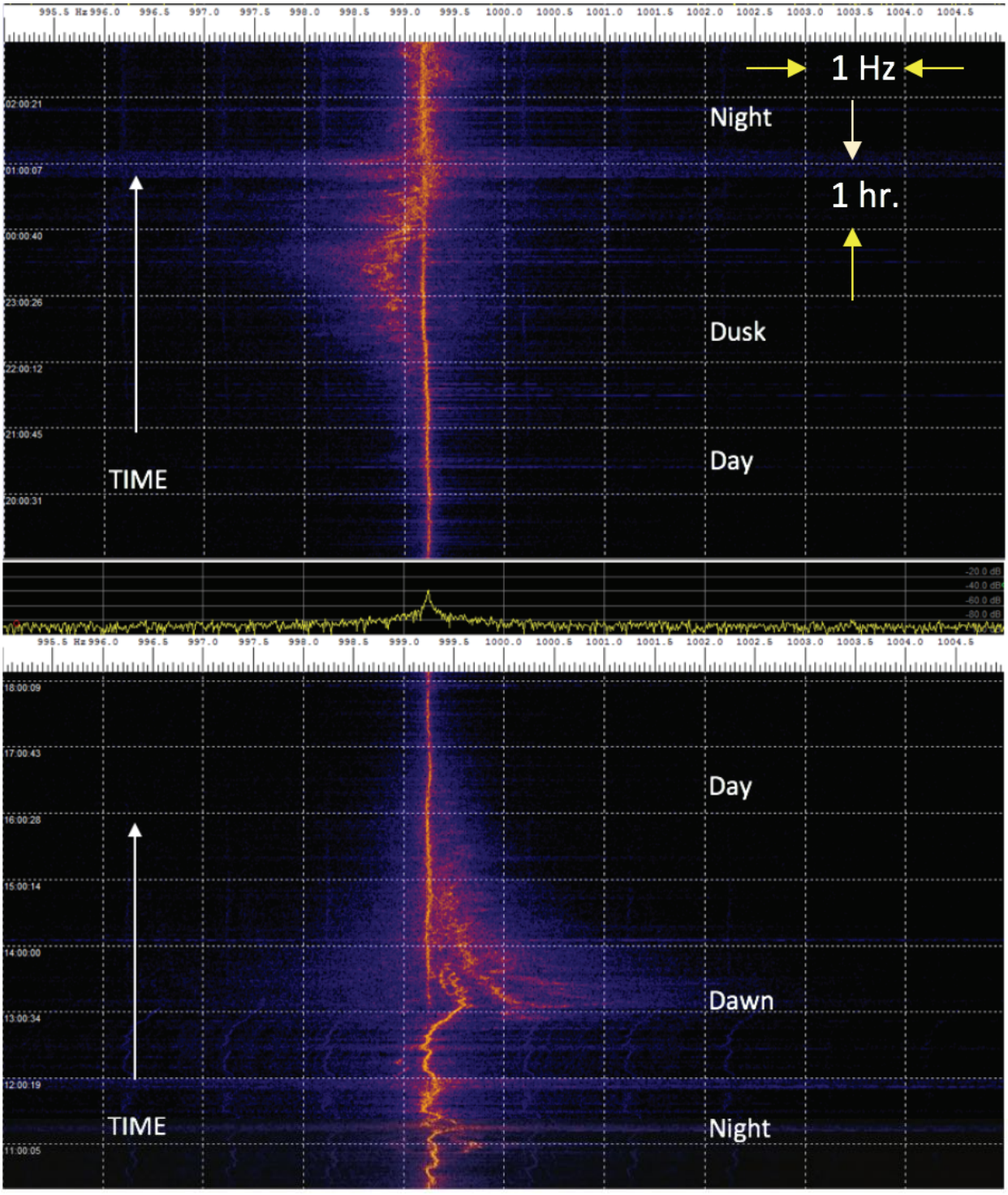

Figure 2 Typical 5 MHz WWV Spectrogram Showing Night, Day, and Transition Behavior

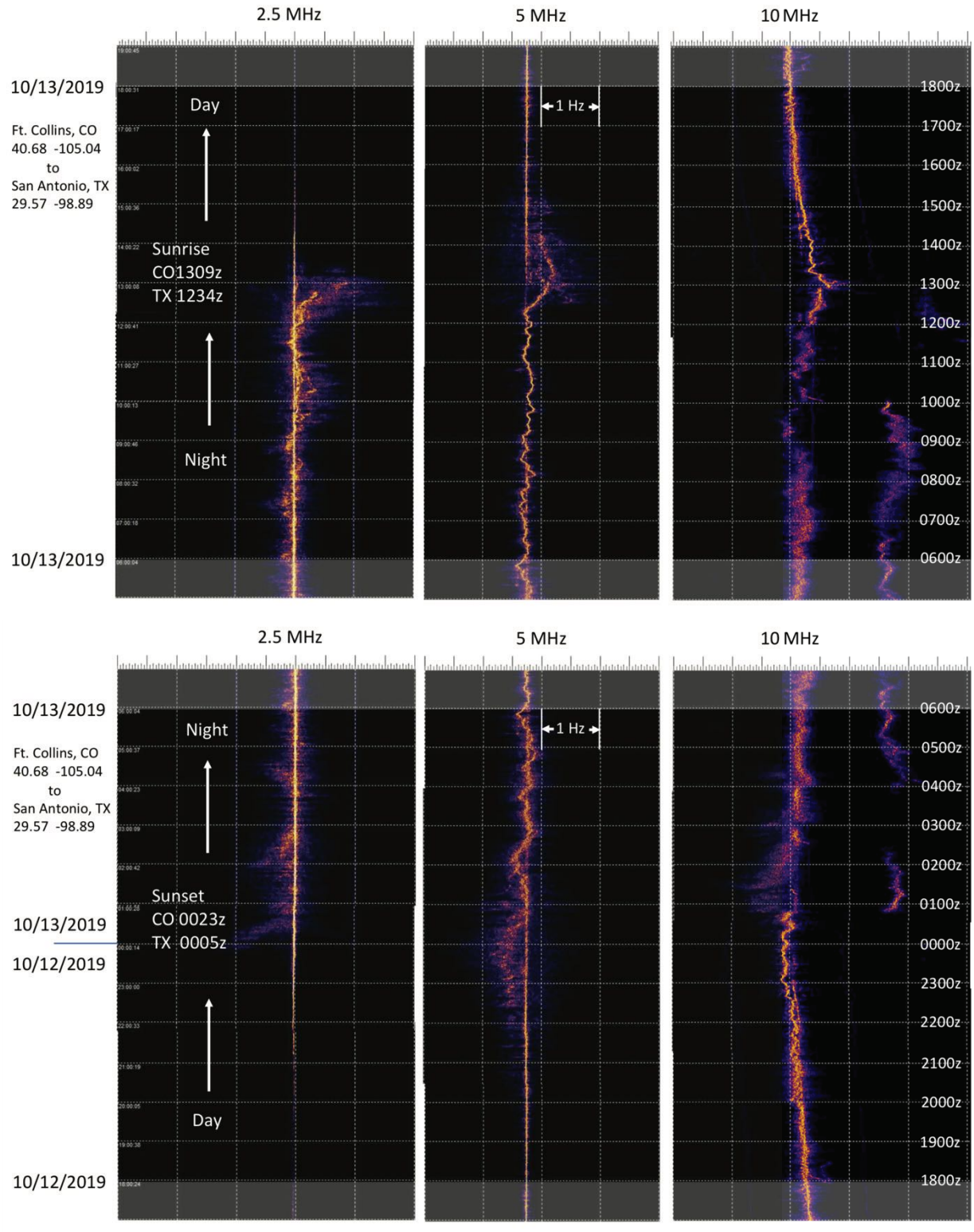

Figure 3 2.5, 5, and 10 MHz WWV for 18z-18z October 12-13, 2019

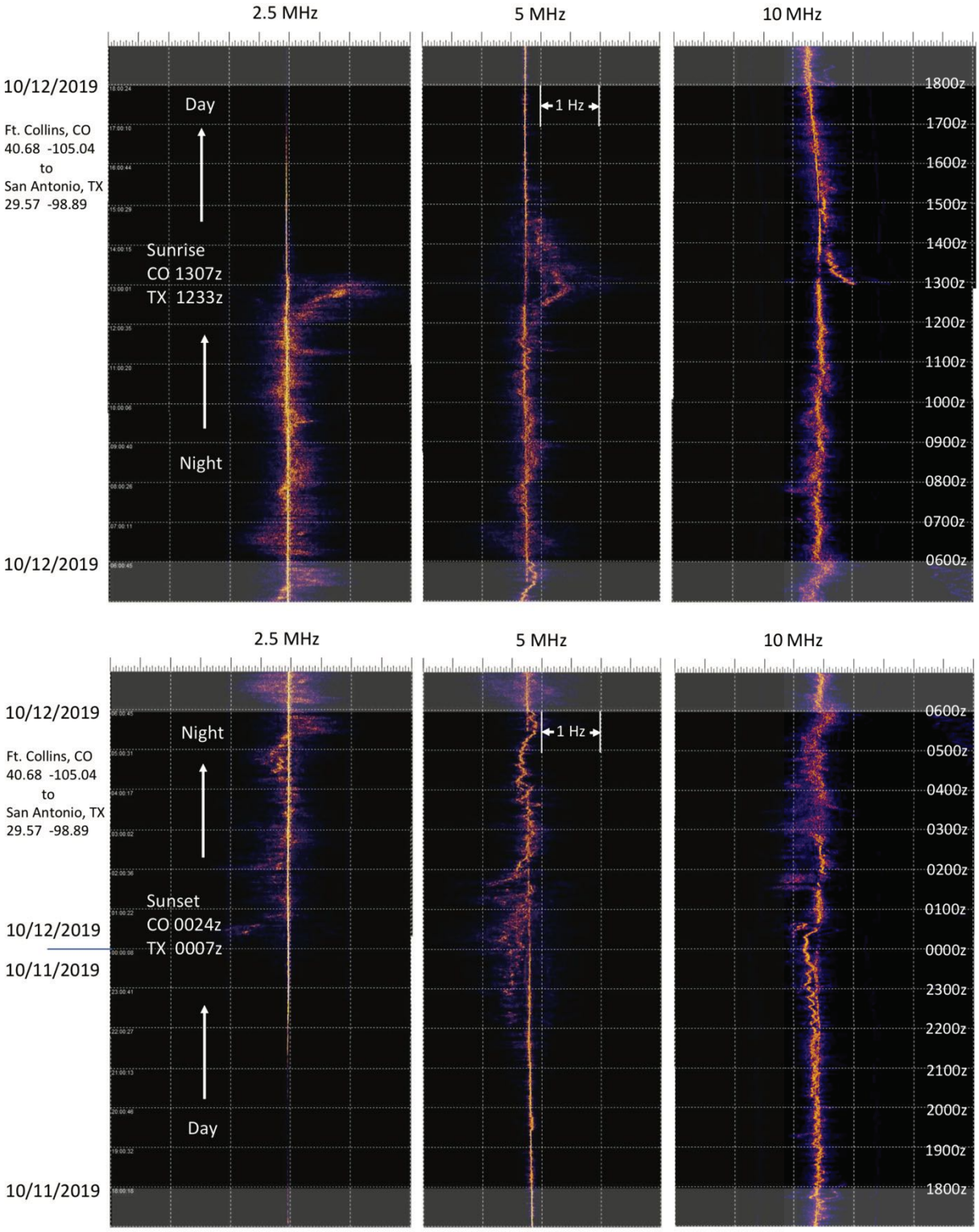

Figure 4 2.5, 5, and 10 MHz WWV for 18z-18z October 11-12, 2019

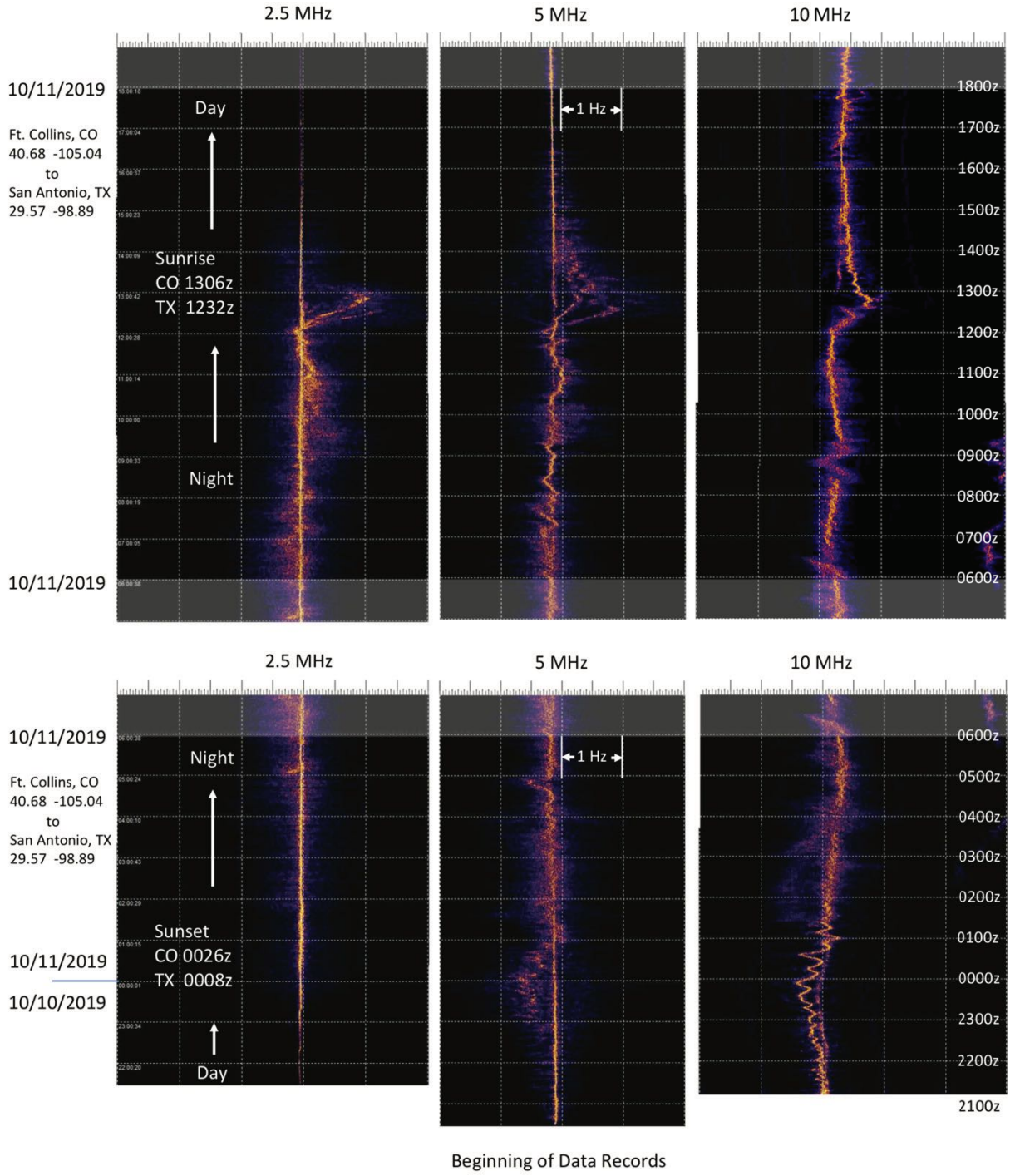

Figure 5 2.5, 5, and 10 MHz WWV for 18z-18z October 10-11, 2019

3. Mode Splitting During Sunrise and Sunset

While there are many interesting nuances and random events with propagation during the middle parts of night and day, the frequency swing and mode splitting behavior that occurs regularly during the dawn transition and occasionally at dusk can provide exceptional insight to the dynamic response of the ionosphere to changing solar illumination. Figure 6 shows additional records of the positive and negative frequency excursions that occur during sunrise and sundown. Horizontal scale is 1 Hz/div in all cases but the vertical time scale may vary.

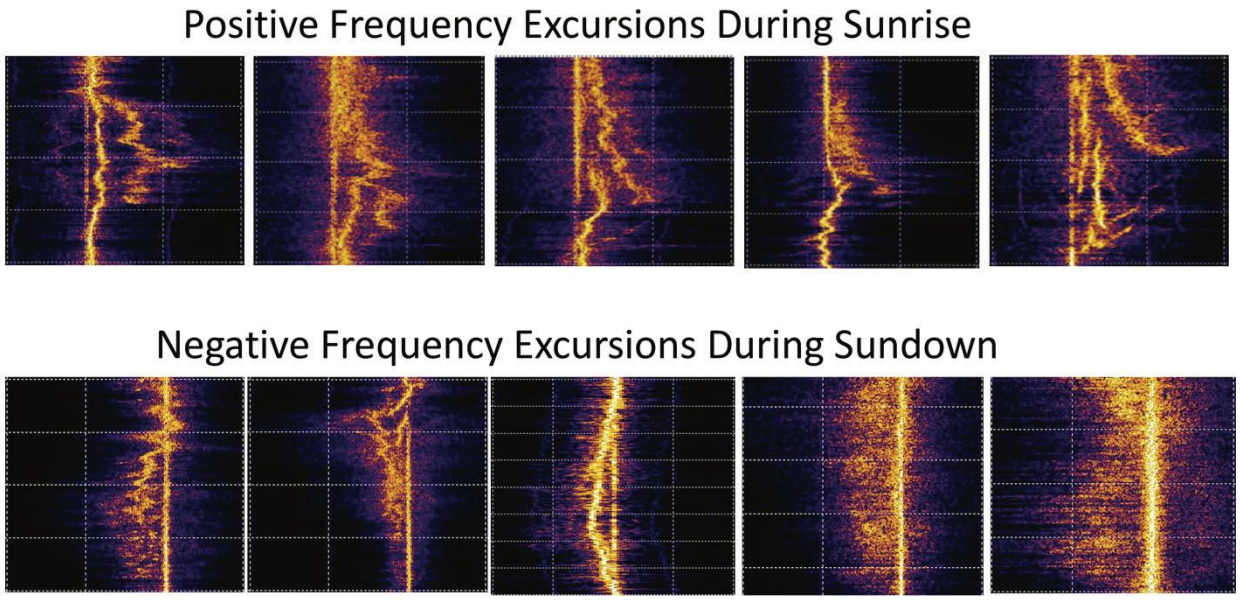

Figure 6 Positive and Negative Frequency Excursions on a WWV-WA5FRF Path During Sunrise and Sundown

In almost all cases there is a constant frequency track that shows little or no frequency displacement, though it can often disappear momentarily while additional higher order modes run amok. During sunrise there can be one to as many as four additional higher order modes. Some modes are present throughout the entire night-day transition showing a half-sine wave shape. Other modes are not present at the beginning of the transition but manifest abruptly part way through. Note that in many cases all of these modes are present at the same time, indicating simultaneous multipath propagation. The negative excursions at sundown show similar behavior but are less radical, probably because of moderation by recombination. Most of the time the evening transition shows only a single extra frequency excursion though occasionally multiple modes manifest.

4. Diffuse Frequency Scatter and AM Sidebands

Many times the modes will print a well defined track whose frequency can be measured as a function of time. But other times the carrier shows a great deal of temporal jitter that can be observed on an oscilloscope. During these times the frequency tracks can take on a fuzzy appearance in a noise band covering a broad frequency range. The two evening captures in the

lower right of Figure 6 are examples. Figure 7 shows an evening capture with an extremely diffuse spectrogram. The pattern is offset low in frequency like the usual evening negative swing but also shows a great deal of diffuse symmetry disposed about it. A non-shifted frequency track continues along the 1000 Hz line throughout the entire track indicating the presence of a non-shifted mode. A GPSDO was used to calibrate the receiver in this recording.

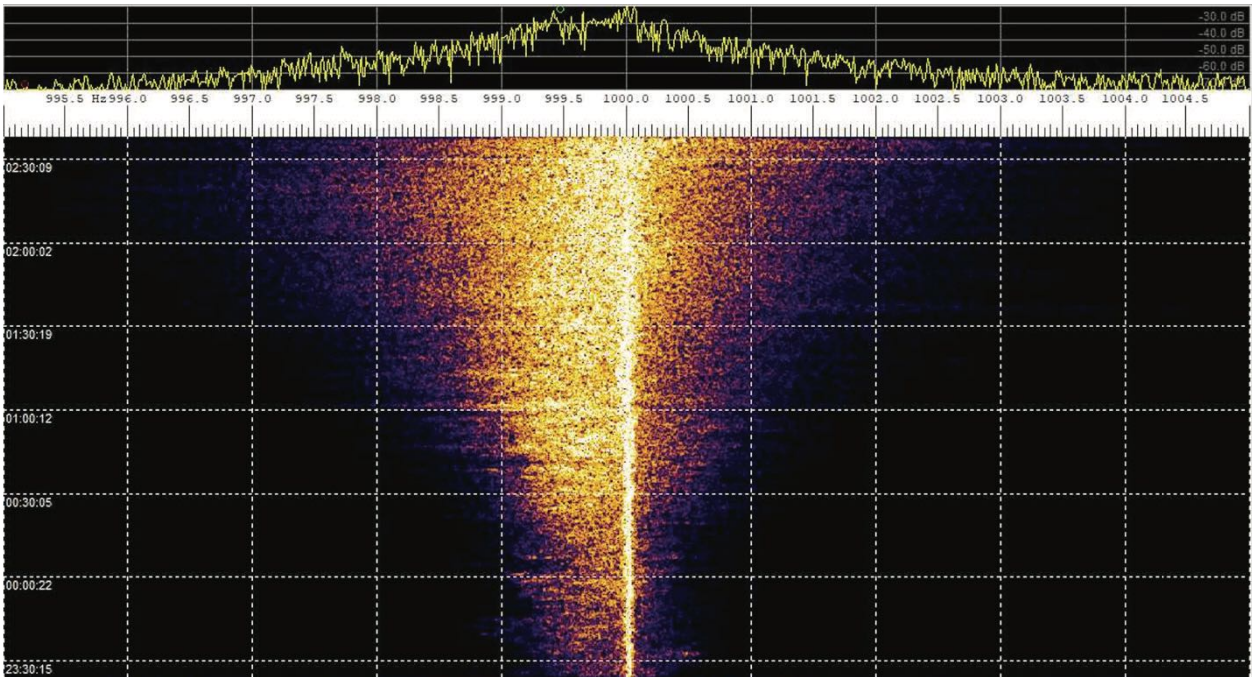

Figure 7 Diffuse Spectrogram Taken During Evening Transition

5. The Ionosphere as an AM and FM Modulator

Insights into ionospheric mechanisms can be gleaned by considering it as an AM and FM modulator. Comparison of the 1 kHz downconverted WWV carrier with a GPSDO stabilized 1 kHz tone from a function generator on a two-channel oscilloscope shows the frequency slewing at dawn and dusk, phase reversals, long term fading and often times rapid amplitude flutter. The combination of rapid amplitude flutter and the symmetry observed in the diffuse spectrograms suggested that at least some of this spectra may actually be AM sidebands resulting from the amplitude fluctuations.

The receiver's automatic gain control AGC is handy for maintaining constant average signal over the course of a long experiment. But it also suppresses amplitude effects if they are what is being studied. Worse, the strong per-second time ticks can pump the AGC, causing amplitude and spectral artifacts. For best data fidelity the receiver AGC should be disabled and signal level set with careful adjustment of the RF gain control.

6. Spectrogram vs. Single Frequency Measurements

There are two basic methods for measuring and displaying frequency data: single frequency and spectral waterfall, or spectrogram. Two popular computer programs within the amateur community for acquiring this type of data are FLDIGI and Spectrum Lab. A single frequency measurement system like FLDIGI is basically an FM demodulator that outputs a serial string of single numbers for the measured value at each time increment. Operational characteristics of the FM demodulator depends on how it is constructed. Characterization measurements on FLDIGI version 4.1.12 showed it to exhibit peak detection and capture effects, similar to the discriminators used in analog FM radios. Within each sample interval the program captures and outputs the frequency of the strongest signal in the passband.

The author built an FM demodulator based on a period counting variation of frequency counting methodology. It had the ability to acquire frequency data at a 100 SPS rate and also had a unique characteristic that allowed identification of the stronger of two multipath modes that were slightly different in frequency. It was useful in studying rapid selective fading when two slightly different frequency modes underwent time dependent interference. As an interference null approached a minimum when the two signals were 180-degrees out of phase the detector exhibited a momentary output swing in frequency. The direction of the swing revealed which frequency had the stronger signal. This behavior was verified in lab experiments using two sinewave generators with precisely controllable frequency and amplitude.

But either FM demodulator could output only a single frequency value per time slot: the value of the strongest signal present in the case of FLDIGI or the average of all signals present weighted by amplitude in the case of the period counter. On the other hand, a spectral analysis program like Spectrum Lab outputs an FFT at each time increment and displays them in waterfall format. It has the distinct advantage of identifying all frequency components present in each sample interval.

Figure 8 shows simultaneous records of 5 MHz WWV taken with all three detection methods during a sunrise transition. All three data representations are formatted to have the same vertical and horizontal scale factors. A comparison shows the obvious advantage of a spectrograph over a single frequency demodulator when mode splitting is present.

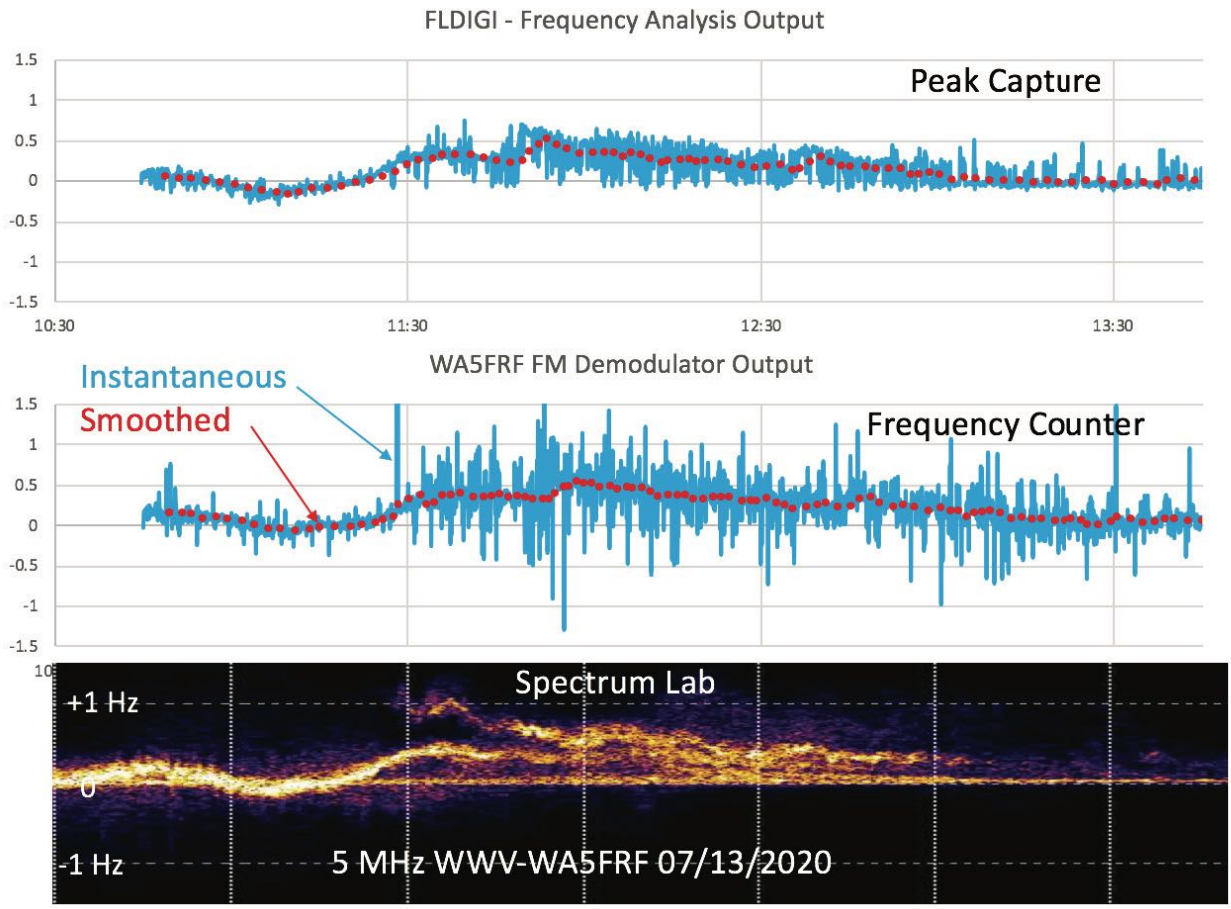

Figure 8 Comparison Between Single Frequency and Spectrogram Displays

The top and middle traces are from the single-valued demodulators. Both instantaneous and smoothed representations are shown. On the bottom is the spectrogram from Spectrum Lab reformatted into a horizontal representation with time amplitude scales matching the other two. The spectrogram shows the presence of three distinct frequency tracks that cannot be deduced from the other two representations. Prior to mode divergence they both followed the spectrogram with fidelity and comparatively low noise. After divergence at approximately 1130z the FLDIGI output showed data spikes corresponding to each of the three modes, depending on relative amplitude. The period counter began showing the bipolar noise spikes that occurred during local amplitude minima.

Each detection type has advantages depending on the task at hand. FLDIGI has become a very popular tool in the Frequency Measurement Test (FMT) community. The period counter proved useful in mode interference analyses that occur on rapid time scales. But for general study of ionospheric phenomenon the spectrogram format provides the most complete data and should be the method of choice for frequency analysis.

III. Precise Timing Measurements on WWV Per-second Ticks to Infer Mode

A. Possible Mode Splitting Mechanisms

The author had hypothesized at least some characteristics of the observed mode splitting on 5 MHz WWV at dawn might be caused by propagation paths using different modes. For a given propagation path between two fixed stations the signal may take one, two, or more hops to get from transmitter to receiver. Multiple hop modes between two fixed stations have longer path lengths because of the extra up-and-down zig-zagging. Path length increases with the number of hops. If all modes use the same ionization height for refraction and that height descends at a given rate, then the longer paths have a faster closure velocity simply because there is more distance change in the same amount of time. The higher closure velocity then creates more Doppler. If conditions permit refraction at the higher angles associated with the multihop modes then the result is simultaneous propagation with the higher order modes showing more Doppler shift according to number of hops. This premise is reinforced by the occurrence of high order modes that abruptly manifest part way through the night-day transition. During the first part of the transition there is insufficient ionization to support the angle required by the mode. When ionization reaches the level required to refract that angle, the mode appears.

Alternate mechanisms for mode splitting certainly exist and might include modes that enter and spend a lot of time within a layer (Pedersen Rays) and frequency shifts from accelerating and decelerating wave speeds. Bill Engelke AB4EJ suggested the possibility of multiple refractions from different layers with different ionization velocities. Of course all of these processes and more may be happening all at once. Additional complications at dawn include appearance or strengthening of the of the D and E layers, splitting of the F layer, and occasional simultaneous presence of WWV and WWVH carriers, each with their own Doppler shifts. The morning transition is a busy time. Sorting out possible contributions requires additional information that can be obtained by designing experiments to test for specific characteristics. It was towards this end that data from a timing experiment was sought.

B. Mode Order Determination through Time-of-Flight Measurement

In order to test the multiple hop idea a method was needed to confirm the presence of simultaneous multiple hop modes. Both measurement of vertical arrival angle and a time of flight measurement were considered. The time of flight measurement was deemed the better choice, and WWV provides convenient time markers via the per-second timing ticks. Since path length increases with number of hops, mode information can be inferred from time of flight. Information on reflection height rates of change, and therefore Doppler shifts, could then be combined with mode data to help analyze spectral recordings.

C. Timing Tick Format

WWV and WWVH transmit audio “ticks” once per second according to published schedules. The timing ticks last 5 mS and are 5 cycles of a 1 kHz sine wave for WWV and 6 cycles of a 1200 Hz

sine wave for WWVH. Figure 9 shows published timing tick data and on-air signals received at WA5FRF displayed on a two-channel oscilloscope. The oscilloscope was connected to the audio outputs of both a 5 MHz receiver (top trace) and a 10 MHz receiver (bottom) set up in AM mode. Horizontal scale factor was 5 mS/div. The top oscilloscope trace shows simultaneous reception of both the 5-cycle tick from WWV followed by the 6-cycle tick from WWVH. The bottom trace shows reception of WWVH only on 10 MHz. The great circle distance is 1350 km from WA5FRF to WWV and 6050 km to WWVH, resulting in a time difference of arrival of about 17 mS. With this station geography there was no problem separating the ticks from WWV and WWVH on the basis of arrival time.

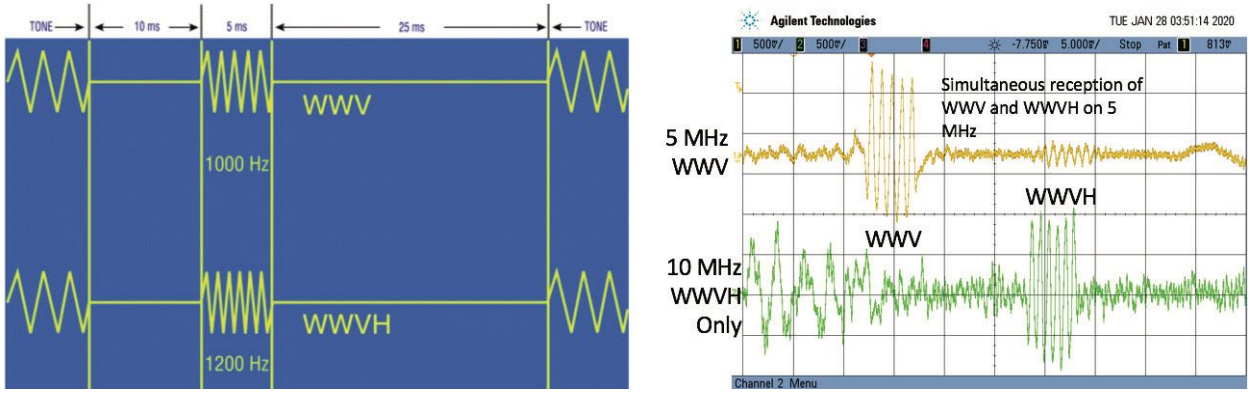

Figure 9 Published Timing Tick Specifications and On-air Received Signals

D. Timing Reference and Receiver Calibration

Three critical elements are required to make precise WWV time-of-flight measurements: an accurate sync pulse referenced to when the pulses are actually launched from WWV, an accurate measurement of the time delay through the receiver, and a consistent On-Time Marker or reference location on the received pulses. A modern GPS Disciplined Oscillator module outputs a 1-second pulse. The rising edge is accurately aligned with the moment of pulse launch from WWV and was used as the oscilloscope sync. The IC-7610 radio is an SDR and the propagation time through the receiver DSP is both lengthy and mode dependent. The propagation delay was measured by feeding a calibration signal into the receiver input and measuring the time delay to the audio output. The test signal was an AM burst generated by a pair of laboratory function generators set up to mimic the WWV timing tick. The delay was measured to be 4.0 mS in AM mode. The published on-time marker for the timing tick is the very beginning of the pulse. However determining the precise instant it actually starts on an oscilloscope display can be difficult, especially under noisy conditions. The middle of the first positive half-cycle of the burst was deemed a much more reliable point of reference and facilitated easy visual measurement using the cursors built into the scope. The first full half cycle of the timing tick was measured at ¾ of a cycle after pulse start. At 1 kHz the period of one cycle is 1.0 mS so this measurement reference is 0.75 uS from the beginning of the pulse. Therefore a time measurement made from sync start to the middle of the first positive half-

cycle on the oscilloscope display required a 4.0 mS correction for receiver delay plus 0.75 mS for the measurement method for a total correction factor of 4.75 mS.

E. Estimated Arrival Times, Superposition of Multiple Modes, and Pulse Broadening

A simplified "flat earth" geometry was used to get a feel for expected times of flight over the 1350 km great circle path from WWV to WA5FRF. The left side of Figure 10 shows the geometry and formulas used to calculate the path distance for 1, 2, and 3 hop modes as a function of virtual reflection height. These distances were converted to time-of-flight and plotted as a function of reflection layer height in the graph on the right. Note that the slopes of the curves increase with mode order. So for a given rate of change in layer height the velocity of path change increases with mode order, predicting more Doppler shift for more hops.

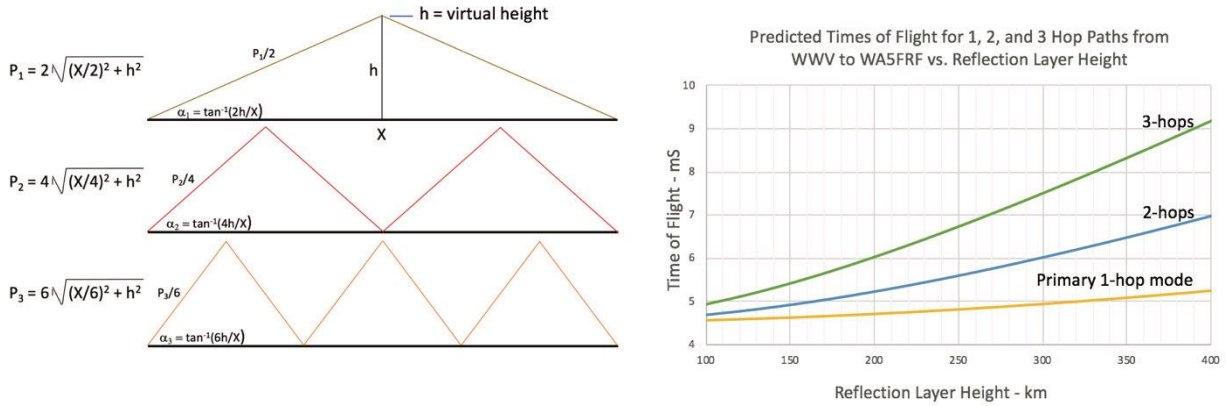

Figure 10 Idealized Geometry used to Estimate Time of Flight vs. Virtual Reflection Height and Predicted TOF for 1, 2, and 3 Hop Modes

At a virtual reflection height of 250 km, the times of flight for 1, 2, and 3 hop modes are 4.80, 5.60, and 6.73 mS respectively. A 2-hop mode would arrive 0.8 mS and a 3 hop mode would arrive 1.93 mS after the primary 1 hop pulse. But the timing tick from WWV is 5 mS long. So under conditions of simultaneous propagation the 2 and 3 hop modes would come down on top of the 1 hop pulse resulting in superposition. At the pulse frequency of 1 kHz, the delayed pulses would arrive about 1 and 2 cycles after the start of the primary pulse.

The superposition of two 5 mS pulses at 1 kHz was modeled in a Spice simulation as a function of phase difference. The upper half of Figure 11 shows results of the simulation for phase differences of 1, 2, and 3 mS, or 1, 2, and 3 complete cycles. For 1 mS delay the resultant consists of the first cycle of the first pulse followed by 4 cycles of the sum of the two, followed by the last cycle of the second pulse. Similarly a 2 mS delay results in 2 cycles from the first, 3 cycles of sum, and 2 cycles from the second. Finally, a 3 mS delay results in 3 cycles from the first, 2 cycles of sum, and 3 cycles from the second. The envelope amplitude shows individual pulse amplitudes as well as the sum. The overall result of the superposition is to lengthen the

resultant pulse by the arrival time difference. Time delays of 1, 2, and 3 mS produced resultant pulses containing 6, 7, and 8 cycles.

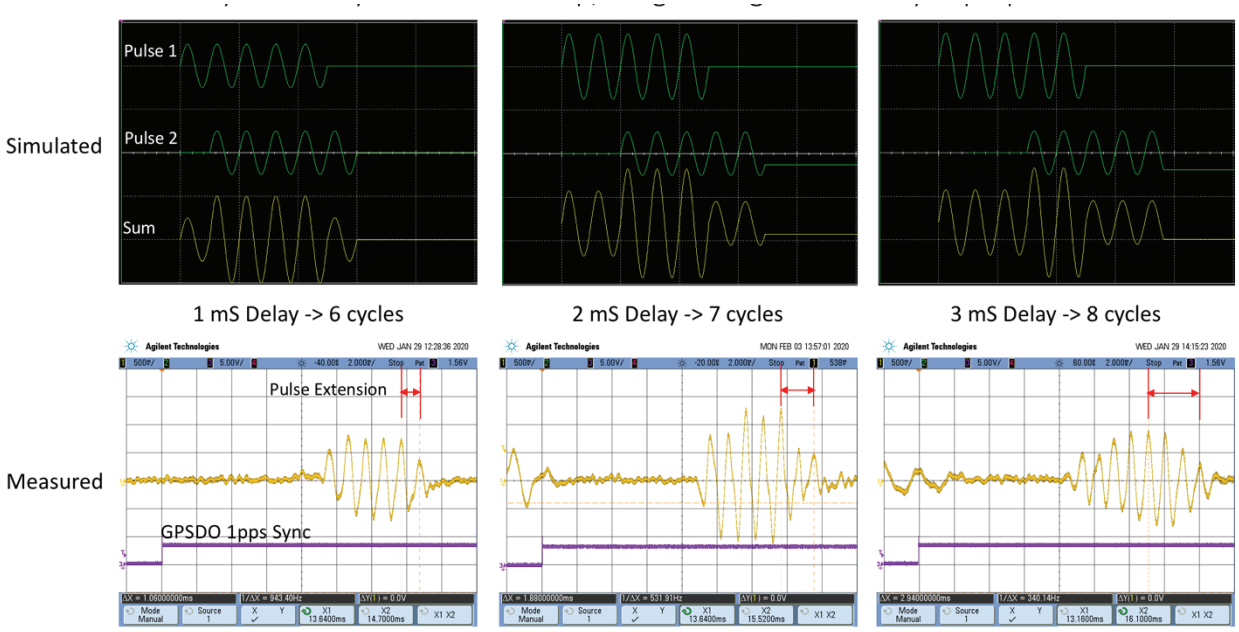

Figure 11 Simulated 5 mS Waveforms with 1, 2, and 3 mS Delayed Superpositions and Recorded On-air WWV Waveforms Showing Similar Characteristics

With this information in hand, it was time to go on the air to see if pulses with these characteristics were actually present during a dawn transition. They were, and oscilloscope recordings of 5 MHz WWV with these characteristic are shown beneath the corresponding simulations in Figure 11. Not shown in the figure are results of superpositions with time differences in-between integral full cycles. These produce more complex waveforms including a central null for the special case of a half-cycle difference. Some of these were observed on the air as well.

F. Measured Data over a Complete Morning Transition

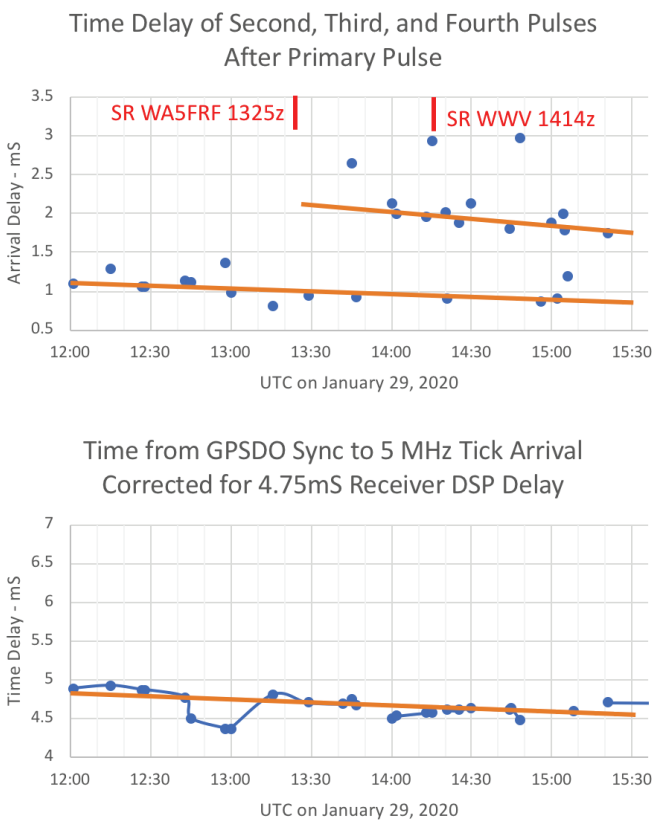

Figure 12 Cluster Plots of Tick Timing Data from January 29, 2020

Data over a 4-hour morning transition was acquired on January 29, 2020. The data was acquired manually by enabling the oscilloscope to trigger on the next available trigger pulse from the GPSDO. Approximately 250 out of the roughly 14,000 possible timing ticks were captured. Primary pulse arrival time was measured at the beginning of the composite pulse. Time delay for a second pulse was obtained from the time extension at the end caused by superposition. Figure 12 shows a cluster plot of the data. The acquired data appeared to cluster in monotonic patterns that were consistent in time and slope with the predicted multihop data of Figure 10 for a specific layer height. Note the higher order modes did not manifest until midway through the transition. This is consistent with data observed on spectrograms.

The timing data supports existence of simultaneous multiple hops and even identified how many hops a particular pulse may have taken. Doppler calculations based on this very sparse data set showed promise in that they predicted frequencies that were present in spectrogram data. Pulse timing data should prove useful in in spectral analyses when use conjunction with other analytical methods and measurements.

G. Correlation with Ray Trace Predictions

Theoretical ray trace data was provided by the HamSCI community to make comparisons with the measured timing data. Published propagation conditions for the day of the experiment were used. Nathaniel Frissell W2NAF provided PHaRLAP ray trace data for a single hop mode at 1200z and for a 2 hop mode at 1324z. Carl Luetzelschwab K9LA provided a Proplab Pro simulation for a 3 hop mode at 1430z. Corresponding data records were available at 1201z, 1329z, and 1444z. Figure 13 shows side by side comparisons between the ray trace predictions and the oscilloscope data records. The measured Times of Flight were consistent with those predicted by the ray trace programs.

Refraction height inferred from idealized geometry consistent PHaRLAP prediction.

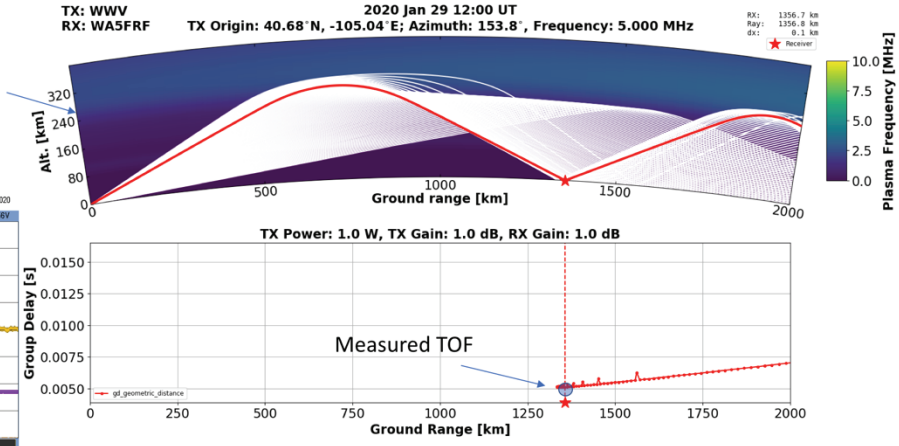

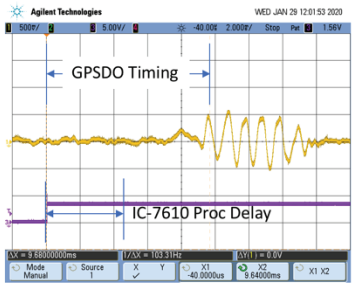

Measured Data

Predicted group delay near 5 mS consistent with measured arrival time of 4.93 mS for primary 1-hop mode at 1201z. T = 9.68 (GPSDO) – 4.75 (IC-7610) = 4.93 mS.

Refraction height inferred from idealized geometry consistent PHaRLAP prediction.

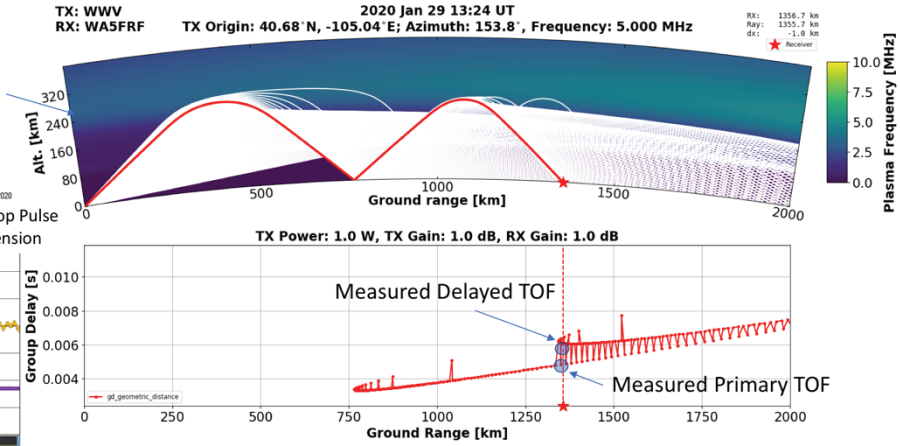

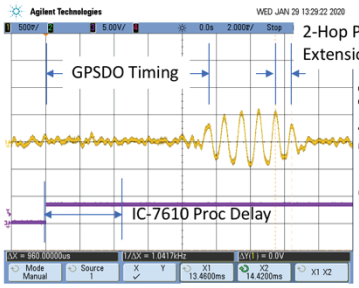

Measured Data

Predicted group delay near 6 mS consistent with measured 2-hop arrival time of 5.67 mS at 1329z. T = 9.46 (GPSDO) – 4.75 (IC-7610) + 0.96 (Extension) = 5.67 mS

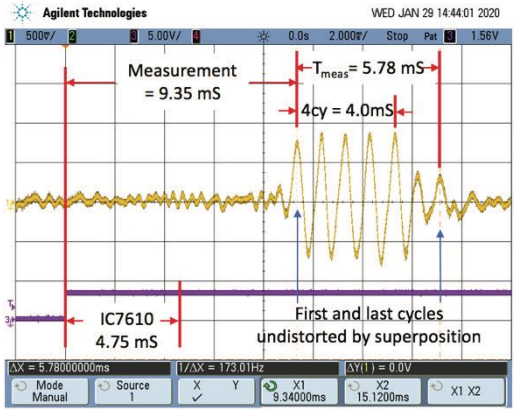

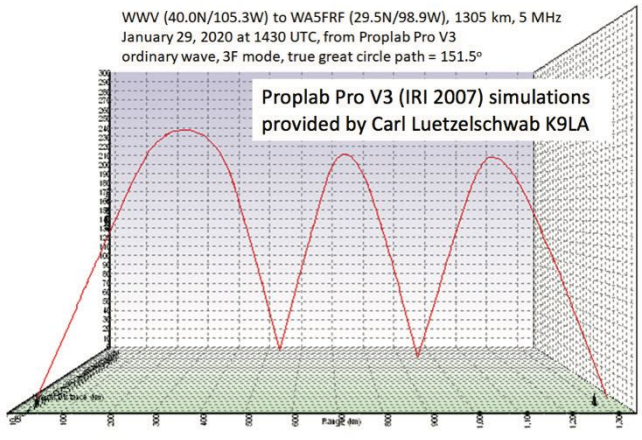

Measured 3F TOF = Leading Edge – IC7610 + T_{meas} – 4 cy
= 9.35 – 4.75 + 5.78 - 4.0 = 6.38 mS

ray trace	mode	elev angle	az angle	total dist in km	time of flight assuming speed of light
3D	3F	49	143.3	1938	6.46 msec

Figure 13 Measured Times of Flight were Consistent with Ray Trace Models

H. Requirement for Automated Data Acquisition and Analysis

This timing experiment is encouraging in that the results are consistent with multihop propagation as predicted by ray trace programs. It is supportive of the premise that at least some aspects of observed spectral mode splitting could come from this form of multipath and should provide a useful analysis tool when used in conjunction with other measurement types and theoretical predictions. The main problems with the experiment reported here are that the acquired data was sparse, manually acquired, and subject to human interpretation. What is needed is an automated data acquisition method that takes data on every available timing tick and then uses a computerized waveform analysis to extract the timing relationships of the overlapping pulses. Much more complete Doppler shift predictions could then be computed from measured path length changes as a function of time. This data then can be compared with an actual spectrogram to see how much of the observed data can be attributed to this effect and what requires additional analyses.

IV. Separation of WWV and WWVH During Simultaneous Reception

A. Spectral Overlap from Simultaneous WWV and WWVH Reception

Simultaneous reception of both Colorado WWV and Hawaii WWVH is a common occurrence at the author's South Texas QTH. Both stations have atomic clock accuracy and ionospheric frequency variations do not amount to more than a very few Hz so the carriers are precisely zero beat and they sound like one station to the ear. The easiest way to tell if you are receiving both is by listening to the time announcements at the top of the minute. The female voice from WWVH comes on first at about 20 seconds before the top of the minute followed by the male voice from WWV about 10 seconds later. Simultaneous reception of both carriers results in superposition of the spectra from both stations in a spectrogram, further complicating an already complicated spectra. Because the carriers use different parts of the ionosphere and come in from very disparate distances their spectra are completely different.

A full analysis of the spectra from WWV is very difficult if the spectra from WWVH cannot be removed. From South Texas separation could be accomplished with directional antennas since angular separation between Hawaii and Colorado is around 50 degrees. But for many stations directly east or west of Colorado the two stations are nearly inline, making an antenna solution virtually impossible. Fortunately the crafters of the WWV/WWVH system had the foresight to build in a solution to separate WWV from WWVH during simultaneous reception.

WWV and WWVH alternate use of 500 and 600 Hz tones in their broadcasts which possess the same frequency accuracy as the carrier. David Kazdan AD8Y recognized the possibility of WWVH interference and suggested use of these tones as a means to separate the two signals. Methods for achieving this separation through deinterlacing the tones were developed by the author and are presented in the following sections.

B. 500 and 600 Hz Tone Interlacing

WWV and WWVH alternately transmit standard tones of 500 and 600 Hz on most (but not all) minutes of each hour. Both stations use both tones in an interlacing scheme described at https://tf.nist.gov/stations/iform.html. The stations swap tones each minute in an even/odd minute order. WWV transmits the 500 Hz tone on even minutes and the 600 Hz tone on odd minutes. WWVH uses the complimentary process. Here is a summary:

Minute	WWV	WWVH
Even	500 Hz	600 Hz
Odd	600 Hz	500 Hz

C. Deinterlace Methods

Numerous separation schemes are possible using one or both tones. Three possible options with increasing complexity and capability are reported below. For these studies the author used a GPSDO stabilized Icom IC-7610, which has dual receivers. In the examples presented here the tone of interest was frequency translated to 1000 Hz so the spectrograms use the same 1000 Hz center frequency, 10 Hz span format used elsewhere in this paper.

1. Interlaced Data using Only One Tone

If a receiver and data recorder are set up to listen to only one tone, WWV and WWVH data appear sequentially in a single waterfall. The individual contributions are recognizable in the alternate-minute composite but only half of the available data for each station is displayed. An example of this method is shown in Figure 14.

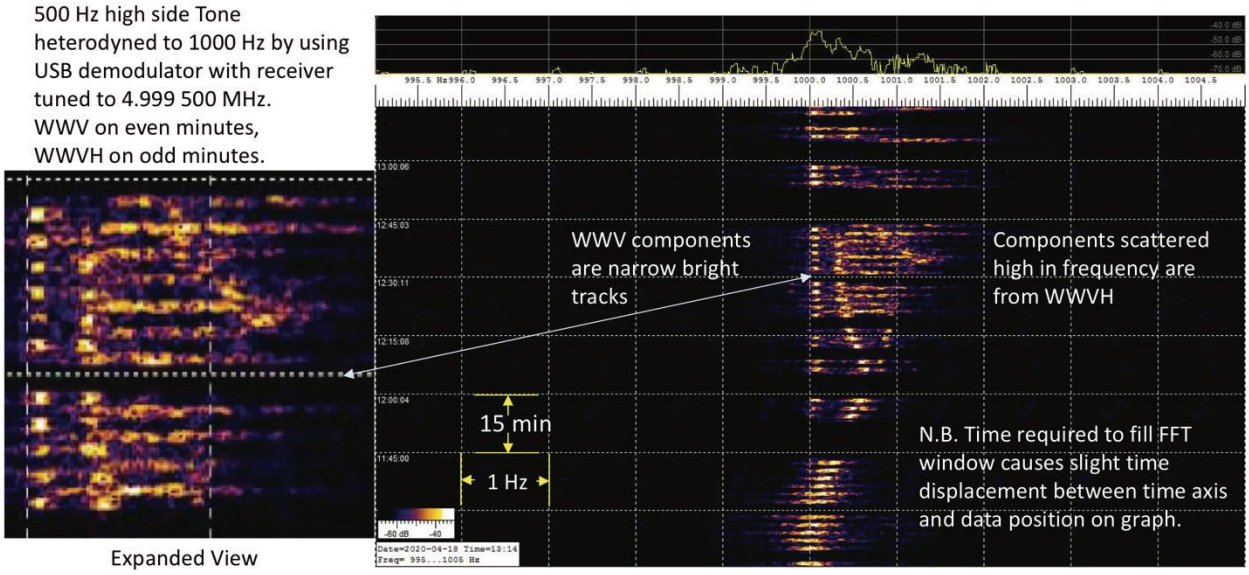

Figure 14 Spectrogram Using a Single Tone. WWV and WWVH Data are Separate but Interlaced

2. WWV or WWVH -only Data Obtained by Muting the Unwanted Tone on Alternate Minutes

This method uses one tone to display only one station at a time by muting the unwanted tone every other minute. It presents sparse data records with 50% of the data missing. The method can be implemented entirely in audio processing with no requirement to control the frequency of either the radio or the analysis program. This method also occurs naturally if only one of the two stations can be heard. An example of this data type is shown in Figure 15.

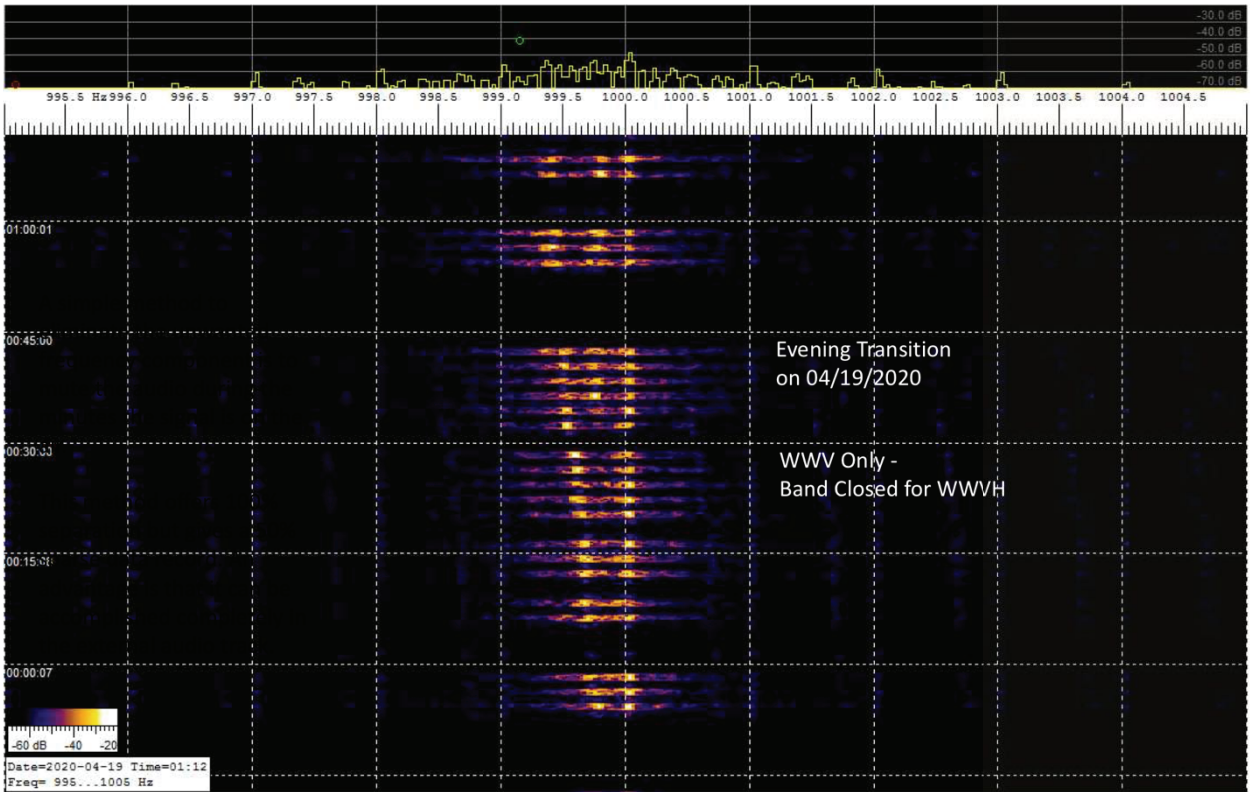

Figure 15 Spectrogram Using a Single Tone but with Alternate Minutes Missing

3. Fully Deinterlaced Processing Placing 100% Continuous Data in Separate Data Records

This method provides full data separation with complete records for both stations but requires two receivers with the ability to change frequency every minute so that one receiver continuously monitors WWV and the other WWVH. Alternatively, full deinterlace can be accomplished if the center frequencies of the data recorders are programmable. A subset of this method is to use only one programmable receiver or data recorder to yield 100% data on only one station. Figure 16 shows data acquired with this method with WWV-only shown on the left side of the figure and WWVH-only on the right. The data traces show all of the transmitted data; the missing minutes are those intentionally not transmitted by WWV. The short gaps between sequential traces are when the tones are muted for the voice announcements prior to the top of each minute. The scale factors were kept the same for both spectrograms so relative amplitude information would be preserved in trace brightness. Mode splitting is clearly present in the WWV trace. The WWVH trace shows a mostly single diffuse mode with a different amplitude profile. Without deinterlacing these spectra would have been superimposed. The mode splitting on WWV would still be evident but blurred by the presence of the WWVH spectra. The spectral information on WWVH would have been unrecognizable.

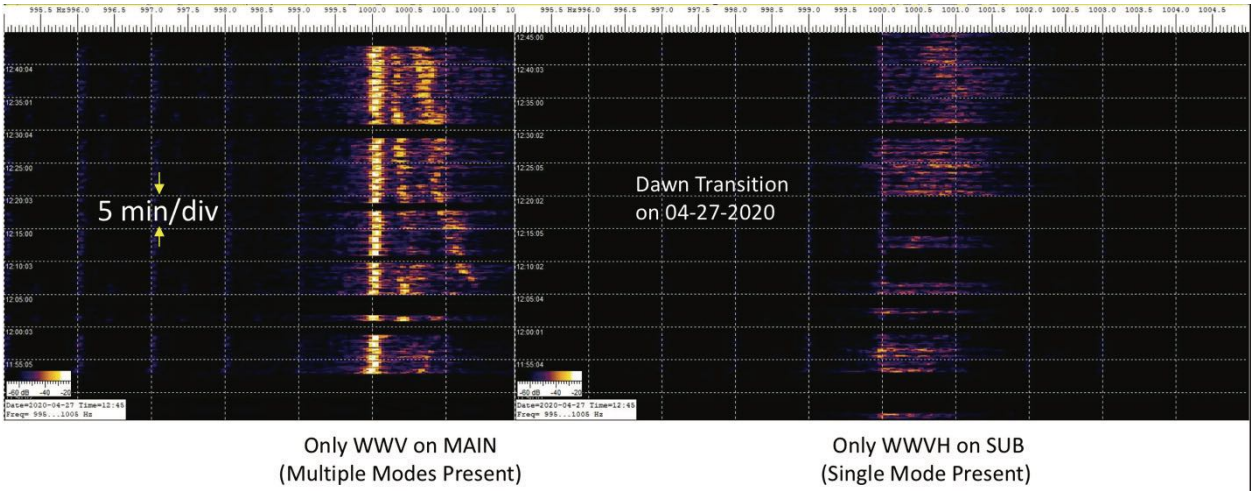

Figure 16 Spectrograms Showing Full Separation with Complete Data Records

Figure 17 shows the setup used to acquire the data for the 5 MHz WWV/WWVH data. Both receivers in an Icom IC-7610 were used and set for USB mode. The Main receiver was set to 4999.5 MHz to translate the 500 Hz tone to 1000 Hz. The Sub receiver was set to 4999.6 MHz to translate the 600 Hz tone to 1000 Hz. Two instances of Spectrum Lab were run on separate laptop computers with Main audio ported to one and SUB audio to the other. Both programs were set up for a 1000 Hz center frequency with a 10 Hz span. The receivers were toggled manually using the CHANGE button prior to the top of each minute throughout the entire course of the experiment.

The left side of the figure shows an automated method to accomplish receiver toggling if an Odd/Even marker can be obtained from an external WWV receiver. This signal could be used, for example, with a microcontroller to toggle the CHANGE command via the CI-V interface.

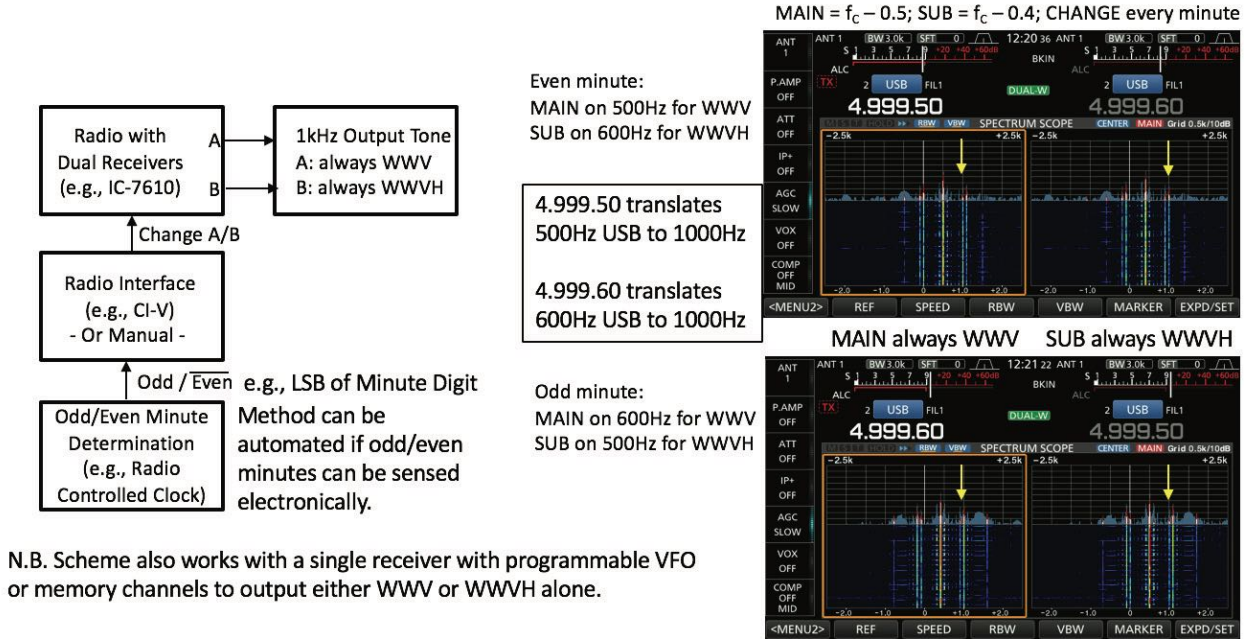

Figure 17 Setup for Full WWV/WWVH Deinterlace Using an Icom IC-7610 Dual Receiver

The right side of the figure shows annotated screen shots of the IC-7610 in the two receive states. The top photo shows MAIN setup for 500 Hz and SUB for 600 Hz. The bottom photo shows reversal after pressing the CHANGE button. The waterfall displays the carriers and both the 500 and 600 Hz tones. Using USB mode and only the high side tones preserves frequency direction sense.

V. Conclusion and Acknowledgements

Ionospheric skywave propagation is a marvelously complex phenomenon with many interesting aspects. The amok times during the morning and evening transitions where apparent frequency and propagation modes run wild is especially fascinating. The underlying physics possess many subtleties which are mysterious to the author in particular and perhaps much of the rest of the amateur radio community in general. But they are still fun to think about and to do so is as engaging as it is addictive. Using different experimental tools can help in deciphering the multiple physical processes involved. The purpose of this paper was to give examples of some of the tools developed for the HamSCI community for the study of ionospheric behavior.

The author would like to thank Nathaniel Frissell W2NAF, Carl Luetzelschwab K9LA, David Kazdan AD8Y, Bill Liles NQ6Z, and Bill Engelke AB4EJ for their valuable insights.